Theory and Experiment in Concert: Templated Synthesis of Amide Rotaxanes, Catenanes, and Knots

Christoph A. Schalley,*[a] Werner Reckien,[b] Sigrid Peyerimhoff,*[b] Bilge Baytekin,[a] and Fritz Vögtle*[a]

Dedicated to Professor Julius Rebek, Jr., on the occasion of his 60th birthday

Abstract: The synthesis of amide rotaxanes, amide catenanes, and trefoil amide knots is based on template effects mediated by hydrogen bonds. While a large body of experimental data is available, in-depth theoretical studies of these template syntheses are virtually unavailable, although they would provide a more profound insight into the exact details of the hydrogen-bonding patterns involved in the formation of these mechanically interlocked species. In this article we present a density functional study of the conformational properties of tetralactam macrocycles and the threading mechanism that produces the immediate precursor for rotaxane and catenane formation. Predictions of the geometries and relative energies made on the basis of semi-empirical AM1 calculations are compared with these results in order to judge the reliability of the simpler approach. Since these calculations yield good agreement with the structural features, they have been used to extend the calculations in order to understand the mechanism of formation of a trefoil dodecaamide knot that has recently been synthesized. The inherent topological chirality of the knot is reflected in the intermediates generated during its formation; these involve helical loops. These loops parallel the rotaxane and catenane wheels with respect to the arrangement of the functional groups that mediate the template effect and may well serve as wheel analogues through which one of the precursor molecules can be threaded. This threading step finally results in the knotted structure. Good agreement between the results of the calculations presented here and experimental findings is achieved.

Keywords: catenanes · density functional calculations · rotaxanes · supramolecular chemistry · template synthesis · trefoil knots

Introduction

Interlocked molecules,[1] that is, rotaxanes, catenanes, and knots, are not only interesting because of their topology and the mechanical bond that holds together two otherwise independent molecules, but also because they form the basis of molecular machinery[2] and consequently may be of practical interest in the future for the realization of miniature switches and logic gates in molecular electronics.[3] One of the most important prerequisites for the realization of such functional species is of course their synthesis, which since the mid-eighties has been much facilitated by template strategies involving noncovalent bonds that mediate the threading of one component into the other.[1,4,5] Of these strategies the most prominent are the coordination of suitably functionalized ligands to metals,[6] π donor–acceptor interactions between electron-rich and electron-poor aromatic systems,[7] and hydrogen bonds to cations,[8] neutral molecules,[9] or anions.[10] Since the design of template effects is still a challenging task and most of these template effects have been found coincidentally, a good understanding of the details of these effects is of prime importance for future research in this field.

In this contribution, we focus on the templated synthesis of amidic rotaxanes, catenanes, and knots.[1d,e,9] The basic structures of these molecules (**1**–**8**) are shown here. The reaction of the extended diamine **1** with one of the acid chlorides **2** or **3** under high dilution results in the synthesis of tetralactam macrocycles **4** or **5**.[9a,11] Catenane **6** is among the side products of the macrocyclization of **4**, while the tre-

[a] Priv.-Doz. Dr. C. A. Schalley, Dipl.-Chem. B. Baytekin, Prof. Dr. F. Vögtle
Kekulé-Institut für Organische Chemie und Biochemie der Universität
Gerhard-Domagk-Str. 1, 53121 Bonn (Germany)
Fax: (+49) 228-735-662
E-mail: c.schalley@uni-bonn.de
voegtle@uni-bonn.de

[b] Dipl.-Chem. W. Reckien, Prof. Dr. S. Peyerimhoff
Institut für Physikalische und Theoretische Chemie der Universität
Wegelerstr. 12, 53115 Bonn (Germany)
Fax: (+49) 228-739-064
E-mail: unt000@uni-bonn.de

 DOI: 10.1002/chem.200400365

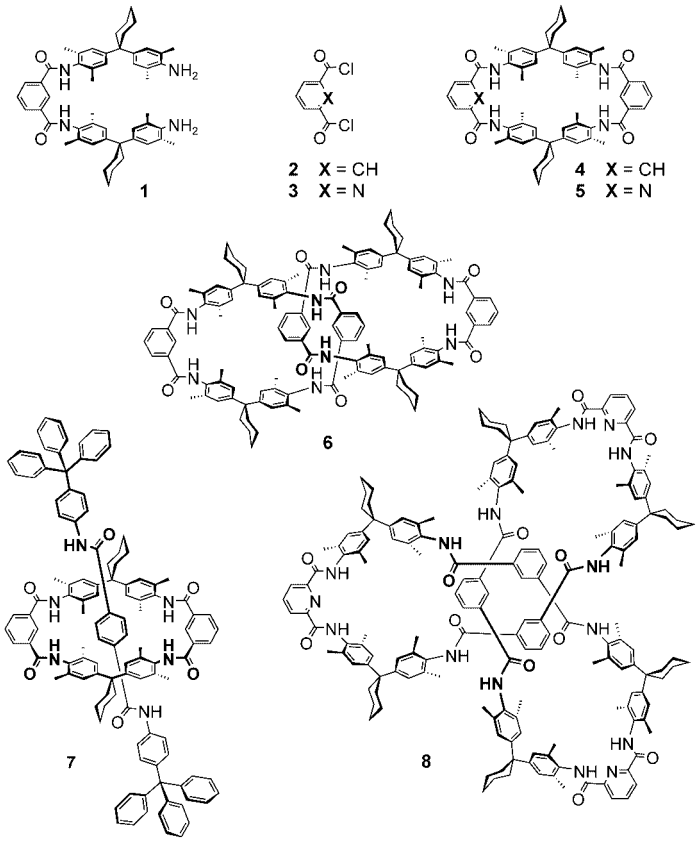

foil dodecaamide knot **8** is formed as a side product in the formation of macrocycle **5**.[12] Rotaxane **7**, which is related to catenane **6** when one considers that the axle bears the same amide functionalities as the second wheel of the catenane, is available through the reaction of terephthaloyl chloride and tritylaniline in the presence of macrocycle **4**. A large variety of similar molecules, which differ with regard to the functional groups attached to the macrocycle or to the structure of the axle's center pieces and stoppers in the case of rotaxanes, have been prepared.

While a significant amount of experimental data is available for these species, a concise theoretical treatment[13] of the template effects operative during their formation has not been reported so far. In particular, the details of the hydrogen bonds that mediate the template synthesis are of interest. In an earlier theoretical study, the strengths of several candidates for such hydrogen-bond motifs were examined by using smaller model compounds.[14] Here, an attempt is made to treat the whole system at a reasonable level of theory by focusing on the structural aspects related to the template effect. Therefore, the conformational flexibility of macrocycles such as **4** and **5** was investigated, and then the noncovalent forces responsible for the formation of catenanes and rotaxanes were analyzed. Finally, the formation of the trefoil amide knot **8** was found to rely on a very similar pattern of hydrogen bonding. The results obtained are compared with the available experimental data in order to evaluate the performance of the theoretical methods employed here.

Abstract in German: *Die Synthese von Amidrotaxanen, Amidcatenanen und dreiblättrigen Amidknotanen beruht auf durch Wasserstoffbrückenbindungen vermittelten Templatsynthesen. Während eine Vielzahl von experimentellen Daten verfügbar ist, gibt es kaum tiefgreifende theoretische Studien dieser Templatsynthesen—und das, obwohl sie einen weit detaillierteren Einblick in die exakten Einzelheiten der Wasserstoffbrückenmuster geben würden, die in der Erzeugung mechanisch verknüpfter Moleküle eine Rolle spielen. Diese Arbeit berichtet daher über eine Dichtefunktionalstudie zu den konformationellen Eigenschaften der Tetralactam-Makrocyclen und zu den Einfädelungsmechanismen, durch die die direkten Vorläufer der Rotaxane und Catenane gebildet werden. Voraussagen von semiempirischen AM1-Rechnungen stimmen mit diesen Ergebnissen hinsichtlich der Strukturen und Energien gut überein. Daher werden die Rechnungen auf semiempirischem Niveau auf den Bildungsmechanismus des Kleeblattknotens ausgedehnt, der kürzlich synthetisiert wurde. Die inhärente topologische Chiralität des Knotens spiegelt sich in den Intermediaten wieder, die in der Synthese durchlaufen werden. Helicale Verschlingungen spielen eine entscheidende Rolle und sind den Rotaxan- und Catenanreifen sehr ähnlich im Hinblick auf die Anordnung der funktionellen Gruppen, die den Templateffekt bewirken. Es besteht eine gute Übereinstimmung der theoretischen mit den experimentellen Daten.*

Computational Methods

One of the problems associated with calculating complex structures such as those examined in this paper is their size and large conformational space. Owing to the computer time required, high-level ab initio methods are necessarily of very limited use for conformational studies of these structures. We have therefore employed a three-step approach. First, force field calculations together with the Monte Carlo algorithm were used to generate and optimize a large number of different structures in order to get an idea of favorable conformations. A selection of the most favorable structures were then reoptimized at the semi-empirical AM1 level of theory. In order to explore how suitable this approach might be, the tetralactam macrocycles served as test cases for a comparison of the semi-empirical and density functional calculations.

Molecular modeling: Conformational searches using the Amber* force field[15] implemented in MacroModel 8.0[16] were performed. In our experience, this method gives excellent results particularly when noncovalent interactions such as hydrogen bonding and van der Waals forces are operative.[17] Depending on the size of the molecule under study and in proportion to its conformational space, between 3000 (for the macrocycles) and 6000 structures (for the knot and its precursors) were generated and optimized during each Monte Carlo simulation, by placing closure bonds in the macrocycles (one of the amide bonds) and the attached cyclohexyl side chains (to allow for ring inversions). While the aromatic rings and the amides were constrained to planarity, all the single bonds (with the exception of the methyl groups, which become oriented properly in the optimization anyway) were selected to allow rotations into other conformations. The two wheels of the catenanes and the axle and wheel of the rotaxanes were treated as independent molecules that can move relative to each other. Note that during the search, the catenanes may convert to structures that consist of two independent macrocycles. Similarly, the rotaxanes may yield a nonthreaded structure and the knot can be converted into a simple nonintertwined macrocycle. This problem is merely a result of the computational algorithm, which treats cyclic molecules like chains by opening one covalent bond (the closure bond). Since such bond clea-

vages do not occur in the real molecule, this, of course, does not have any chemical implications. In order to prevent this, it is wise to choose amide bonds at the periphery as closure bonds with a maximum closure distance of 2 Å. For each optimization the number of iterations was set to 10000 in order to generate fully converged structures. The energy range of the structures to be stored in the output file was set to 50 kJ mol^{-1} above the lowest energy conformer. Since this protocol still does not probe the complete conformational space, such calculations were repeated with other starting geometries. For example, initial guesses for the knot precursors were derived from fully extended rodlike structures as well as from the knot by cutting open one of the amide bonds without any other change to the structure.

AM1 calculations: The energetically most favorable conformations derived from the Monte Carlo simulations were then reoptimized at the semi-empirical AM1 level of theory as implemented in the MOPAC version delivered with the CaChe 5.0 program.[18] Some structures were also optimized with Gaussian 98[19] to compare the two programs; these gave the same results. Generally, good agreement between the force field and the AM1 calculations was obtained for the structures and relative energies of the conformers.

Density functional calculations: To compare the semi-empirical calculations with quantum chemical results, geometry optimizations for the smaller structures were performed at the density functional (DFT) level by using the TURBOMOLE 5.4 program.[20] The density functional optimizations were performed with the B3LYP[21] functional and a basis of double-zeta quality that includes d-polarization functions (DZP). Furthermore, the B-P functional[22] in the RI approach[23] was also employed for comparison by using the SV(P) basis as implemented in the TURBOMOLE set of programs. For single-point calculations on the threaded axle/wheel complex, the BHLYP functional[24] and DZP basis were used, because previous calculations have shown that hydrogen-bonding energies are described more realistically with this functional.[14] The basis set superposition error (BSSE) is in these cases considered as a counterpoise correction.[25] Geometry optimizations that employ the DFT approach consume a lot of computer time, even for the smaller structures, such as the tetralactam macrocycles, under study here. Therefore, cyclohexyl rings were replaced by methylene groups in the DFT calculations. These groups are not expected to have a significant effect on the relative energies of the amide group conformations (see discussion below). In order to study the conformational stability of the macrocycle, the transition structures for the rotation of the amide groups were optimized at the AM1 level followed by B3LYP single-point calculations on the respective AM1 geometries.

One problem to be borne in mind when comparing experiment and theory is the fact that measurements are conducted in solution. For most experiments, dichloromethane was used, because it does not interfere significantly with hydrogen bonding. Generally, one assumes that the influence of such weakly polarized solvents is quite small and that such a situation in solution is sufficiently close to the gas-phase calculations discussed here. On the other hand, strongly polar solvents are expected to affect hydrogen bonds quite markedly. For this reason, we have simulated the solvent by incorporating dielectric constants ε into additional DFT calculations (DZP/BHLYP) by using the COSMO (conductor-like screening model)[26] implementation in TURBOMOLE. The values chosen for ε correspond to the gas phase ($\varepsilon = 1.0$), chloroform ($\varepsilon = 4.9$), dichloromethane ($\varepsilon = 8.9$), dimethyl sulfoxide ($\varepsilon = 46.7$), and, for comparison, $\varepsilon = \infty$. These calculations were carried out by using the following default parameters: the number of points per atom in the cavity construction (nppa) = 1082, the number of segments (groups of points) per atom (nspa) = 92, the distance threshold for elements of matrix **A** (disex) = 10.0 Å, the distance to the outer solvent sphere (rsolv) = 1.3 Å, and the distance of the extra solvent sphere (routf) = 0.85 Å. For the generation of the cavity the atomic radii were chosen as 1.17 times the van der Waals radii (1.9890 Å for C, 1.7784 Å for O, 1.8135 Å for N, and 1.4040 Å for H).

Results and Discussion

Conformational flexibility of the tetralactam macrocycle: For the density functional calculations performed in order to assess the conformations of the tetralactam macrocycles, analogue **9**, which lacks the two cyclohexyl side groups, was employed. Five different conformers **9.1**–**9.5** of this macrocycle were examined by density functional methods (Figure 1).

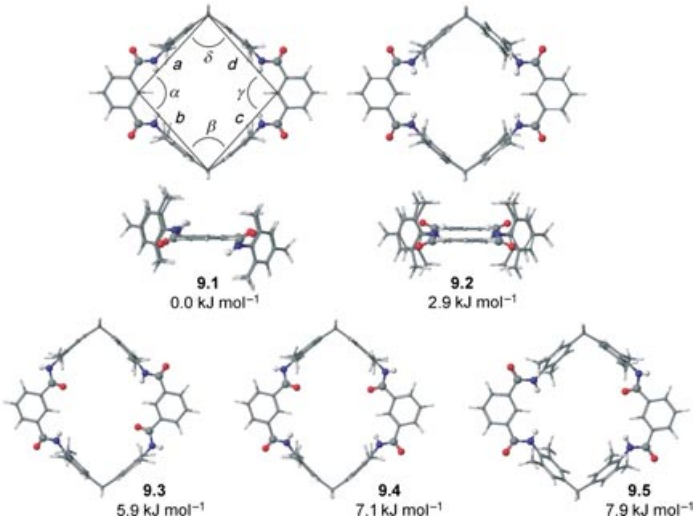

Figure 1. Five conformers **9.1**–**9.5** of tetralactam macrocycle **9** optimized with the B3LYP density functional hybrid and a DZP basis. Structures **9.1** and **9.2** are also viewed from the side along the line connecting the two isophthalic dicarboxamide moieties in order to show the NH groups above and below the macrocycle plane. The relative energies of these conformations are very similar to each other. The definitions of the geometry parameters used in Table 1 for characterizing the cavity sizes and shapes are shown in the structure of **9.1**.

Although the macrocycles bear six aromatic rings connected by either methylene groups or amides with their rather high rotational barrier, they exhibit some conformational flexibility. We can distinguish an "*in*-conformation" of the amide groups with the NH proton pointing into the cavity of the macrocycle and an "*out*-conformation", in which the amide proton is rotated out of the cavity while the carbonyl group points inwards. This change in conformation does not significantly alter the relative energies of the conformers (Figure 1 and Table 1). The energetically preferred (**9.1**) and least favorable (**9.5**) structures differ by less than 9 kJ mol^{-1}. We attempted to optimize the geometry of several other structures with two, three, or even four adjacent amide groups in the *out*-orientation; however, such structures were found not to be local minima.

A closer look reveals that the amide NH protons are not exactly coplanar with the aromatic ring of the isophthalic dicarboxamide parts. Consequently, the two all-*in* conformations **9.1** and **9.2** differ in the directions of the NH groups relative to the macrocycle plane (side views in Figure 1). In **9.1**, both isophthalic dicarboxamide moieties are connected to one amide group directed below the plane and to one directed above the plane. In **9.2**, the two amide NH groups of each isophthalic dicarboxamide point in the same direction. These results suggest that two barriers to the conformational change of an amide group exist. The first barrier for the transition from **9.1** to **9.2**, in which the amide switches be-

Table 1. Relative energies [kJ mol^{-1}] and geometry parameters for the cavities [distances in Å, angles in degrees, see Figure 1 for their definition] of five different tetralactam macrocycle conformations **9.1**–**9.5** as calculated at the B3LYP, the B-P RIDFT, and the AM1 levels of theory.

	9.1			**9.2**			**9.3**			**9.4**			**9.5**		
	B3LYP	B-P RIDFT	AM1	B3LYP	B-P RIDFT	AM1	B3LYP	B-P RIDFT	AM1	B3LYP	B-P RIDFT	AM1	B3LYP	B-P	AM1 RIDFT
E_{rel} [kJ mol^{-1}]	0.0	0.0	0.0	2.9	3.0	3.0	5.7	6.4	2.5	7.2	7.9	3.2	8.2	8.5	4.9
a [Å]	8.45	8.48	8.40	8.46	8.49	8.41	8.39	8.41	8.35	8.32	8.36	8.27	8.57	8.60	8.52
b [Å]	8.45	8.50	8.40	[a]	[a]	[a]	8.68	8.75	8.48	8.76	8.81	8.59	8.50	8.55	8.42
c [Å]	[a]	[a]	[a]	[a]	[a]	[a]	[a]	[a]	[a]	8.75	8.81	8.59	8.27	8.29	8.29
d [Å]	[a]	[a]	[a]	[a]	[a]	[a]	[a]	[a]	[a]	8.33	8.35	8.27	8.59	8.65	8.46
α [°]	96.4	96.4	97.1	95.9	95.5	96.1	111.9	111.8	108.0	111.0	111.1	107.4	101.8	102.0	99.8
β [°]	83.6	83.6	82.9	84.1	84.5	83.9	68.1	68.2	72.0	71.0	66.7	71.0	78.3	78.3	80.0
γ [°]	[a]	[a]	[a]	[a]	[a]	[a]	[a]	[a]	[a]	111.0	111.3	107.5	103.6	103.7	101.4
δ [°]	[a]	[a]	[a]	[a]	[a]	[a]	[a]	[a]	[a]	71.0	70.9	74.2	76.2	76.1	78.5

[a] For symmetry reasons, $a=c$, $b=d$ ($a=b=c=d$ for **9.2**), $\alpha=\gamma$, and $\beta=\delta$.

tween the two orientations above and below the macrocycle plane, but in which the NH remains oriented towards the cavity, is computed to be approximately 4 kJ mol^{-1}. It is unlikely that this process occurs simultaneously for two or more amide groups. The second barrier represents the transition of one of the amide groups from an *in*- to an *out*-conformation and requires approximately 29 kJ mol^{-1} of activation energy according to the calculation. Both barriers are rather low. Furthermore, calculations that model the solvent for dielectric constants ε ranging from 1.0 to 46.7 (DMSO) show the solvent polarity to have very little influence (less than 2 kJ mol^{-1}) on the relative stability of the various conformations of the macrocycles listed in Table 1. These calculations predict conformations **9.1**–**9.5** to be in equilibrium at room temperature in solution.

The four dimethylphenyl rings of the two diamine subunits are perpendicular to the plane of the tetralactam macrocycle for all the conformers studied so that a rhomboid cavity as defined in Figure 1 is formed whose dimensions are characteristic of each conformer. The distances a, b, c, and d and the angles α, β, γ, and δ are summarized in Table 1. Taking into account the ease with which transitions between the five conformers occur, the cavity of the macrocycle may well adapt to some extent to the sizes and shapes of potential guests.

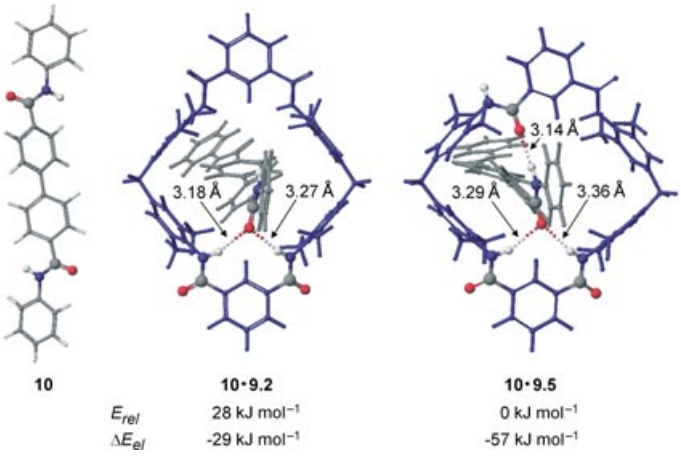

Figure 2. From left to right: truncated axle **10** and structures of complexes **10·9.2** and **10·9.5** as optimized at the DFT level of theory. Dotted lines represent hydrogen bonds between the two components. Energies are the relative energies (E_{rel}) of the two complexes and the electronic energy differences relative to the two separate components (ΔE_{el}). The lengths of the hydrogen bonds (from donor to acceptor heteroatom) are given.

Complexes of axle and wheel—how to achieve a threaded geometry: After examining favorable conformations of the wheel, the next step towards an analysis of the template mechanism that mediates rotaxane formation is to study the interaction between the tetralactam macrocycle and the axle. In order to make economic use of computer time, we placed the truncated axle **10** (Figure 2) into the macrocycle cavity; this molecule corresponds to a typical[27] amide rotaxane axle without the bulky stopper groups. If **10** is inserted into the all-*in*-conformer **9.2**, in which the two amide NH protons of each isophthalic dicarboxamide are directed towards the same side of the macrocycle, two hydrogen bridges are formed between these NH groups and the oxygen atom of one carbonyl group of the axle (Figure 2). BHLYP single-point calculations using the B-P RIDFT optimized structures provide a value of approximately 29 kJ mol^{-1} by which the complex that forms a twofold (bifurcated) hydrogen bridge is lower in energy than its separate components. The complex of **10** and **9.5** is an alternative, in which one of the amide groups of the macrocycle is in an *out*-conformation so that one carbonyl group points into the cavity. Although **9.5** is calculated to be the least favorable conformer of **9**, the resulting complex **10·9.5** is lower in energy than the two separate components by 57 kJ mol^{-1}, owing to the formation of a third hydrogen bond that connects the NH of the axle amide group to the carbonyl oxygen atom of the inverted amide within the macrocycle (Figure 2). Consequently, this structure, which has a total of three hydrogen bonds, is more favorable than its analogue by approximately 28 kJ mol^{-1}. A more detailed analysis of these binding energies shows that about 13 kJ mol^{-1} are consumed in the small changes to the geometry of the components that are needed to realize a perfect geometry for binding. In other words, the lowering in the electronic energy due solely to hydrogen bonding would be 42 kJ mol^{-1} for **10·9.2** and 70 kJ mol^{-1} for **10·9.5**. These values are in good agreement with calculations on smaller model systems that have been reported previously,[14] which have shown a twofold hydrogen bridge to be approximately 1.5 times

stronger than a single hydrogen bridge. On the basis of the value of 42 kJ mol^{-1} for the twofold hydrogen bridge determined for **10·9.2**, one can thus estimate the third single hydrogen bond in **10·9.5** to provide an additional binding energy of approximately 28 kJ mol^{-1}, which together with 42 kJ mol^{-1} provided by the two-old hydrogen bond also present in **10·9.5**, results in a total of 70 kJ mol^{-1}. The other conformations of macrocycle **9** are not suitable for binding **10** as the guest inside their cavities and a transition to either **9.2** or **9.5** would be required for a favorable arrangement of the amide groups. On the basis of this "back-bonding" motif the calculations suggest secondary amides to be much more suitable as guests for templating rotaxane synthesis than other carbonyl compounds, such as tertiary amides, esters, or ketones, which are unable to form the third hydrogen bond owing to the lack of amide NH.

One might speculate whether π–π stacking interactions between the axle and the macrocycle play an important role, because aromatic rings of both components can be oriented in a parallel fashion. However, the distance of about 5 Å between these rings is much larger than the usual distance of about 3.5 Å between stacked aromatic rings. Since DFT methods might not treat these interactions correctly, MP2 calculations in the RI approximation,[28] as implemented in TURBOMOLE 5.4 (TZVP basis), were carried out. They result in π–π stacking interactions in the order of 5 kJ mol^{-1} when the counterpoise correction is included and thus confirm that stacking interactions do not play a significant role in the binding of the axle.

The experimental results are in good agreement with these calculations. First, the hydrogen-bonding patterns observed in X-ray crystal structures of rotaxanes involve all three hydrogen bonds as calculated.[29] Then, the flexibility of the amide groups to interconvert between *in*- and *out*-conformations and their hydrogen-bonding capability is reflected experimentally in the recently reported deslipping kinetics of rotaxanes bearing ester groups in the axle.[17c] These rotaxanes show a distinct solvent effect on the rate with which the wheel slips over one of the stoppers and liberates the two components. In dimethyl sulfoxide (DMSO), a highly competitive solvent, deslipping is observed for a representative rotaxane with a half-life of 560 h at 373 K, while only a lower limit of 25 000 h could be estimated for the half-life of the same rotaxane in a noncompetitive solvent such as tetrachloroethane (TCE) at the same temperature. This dramatic solvent effect is attributed to the formation of hydrogen bonds between the wheel and the axle in TCE, while DMSO efficiently competes and forms hydrogen bonds with the wheel itself. Since the cavity is occupied by the rotaxane axle, the amide groups need to rotate into an *out*-conformation in order to bind the solvent molecules. Finally, experiments confirm that secondary amides bind significantly more strongly than tertiary amides, ketones, acid chlorides, or esters.[27]

However, the absolute binding constants in dichloromethane solution amount to $K = 200$–$300\,\mathrm{M}^{-1}$ for secondary amides, which translates into a binding energy of approximately 14 kJ mol^{-1} at room temperature, a value significantly lower than those calculated here. This difference may be attributed to solvation and entropic effects. It is almost impossible to estimate the entropic effects for the solvated species under study. On one hand, one might argue that two independent molecules form a complex causing the entropy to decrease, owing to the higher order generated through complex formation. On the other hand, it is not unreasonable to assume that the wheel cavity is filled with solvent molecules that are liberated upon binding of the axle. If, for example, two molecules of dichloromethane occupy the cavity, one would form an axle–wheel complex plus two molecules of dichloromethane during complex formation. Such effects have nicely been examined for the Rebek softballs,[30] which encapsulate two molecules of benzene. Larger guests are driven into the cavity of the softballs through the entropically favorable release of two solvent molecules. Consequently, the entropic contributions may even affect complex formation positively. Since we do not know the details of solvation, it is thus not easy to provide a realistic estimation of the entropic effects by theory here.

Nevertheless, the effects of solvation can be taken into account in the calculations by modeling the solvents through their dielectric constants (ε) by using the COSMO algorithm (see the Computational Methods section). Table 2 provides the binding energies (including BSSE)[31] for **10·9.2** and **10·9.5**, as calculated with different values of ε. As expected, higher solvent polarities cause a decrease in binding energies for both complexes. The calculated value of 14.2 kJ mol^{-1} for **10·9.5** in dichloromethane ($\varepsilon = 8.9$) is in excellent agreement with experiment (14 kJ mol^{-1}). However, the negative binding energy of −9.6 kJ mol^{-1} calculated for **10·9.2** in dichloromethane does not correspond to a bound species. Most importantly, the difference between the binding energies of **10·9.2** and **10·9.5** does not change much irrespective of the dielectric constant used for these calculations. It is calculated to be approximately 28 kJ mol^{-1} in the gas phase ($\varepsilon = 1.0$), and approximately 22 kJ mol^{-1} for $\varepsilon = \infty$. This suggests that complex **10·9.5** with its three hydrogen bonds between the axle and the wheel is more stable than **10·9.2** in a wide range of solvents.

Table 2. Binding energies [kJ mol^{-1}] calculated for **10·9.2** and **10·9.5** for different dielectric constants with the COSMO algorithm implemented in TURBOMOLE.

ε	1.0	2.0	4.9	8.9	46.7	∞
solvent	gas phase		$CHCl_3$	CH_2Cl_2	DMSO	
10·9.2	28.7	12.2	−3.3	−9.6	−16.8	−17.2
10·9.5	56.7	38.0	21.1	14.2	6.4	5.2
ΔE	28.0	25.8	24.4	23.8	23.2	22.4

A transition structure for the threading process has not been calculated, owing to the floppy nature of the complex formed. Also, a potential effect of the chloride anions formed during the synthesis of the rotaxanes is likely to need a more in-depth investigation, although so far there has been no indication that they play a pivotal role. They are not found in any of the available crystal structures of amidic rotaxanes or catenanes, nor does the addition of tetrabutylammonium chloride to a solution of a derivative of

catenane **6** change its NMR spectra significantly. For the time being, these two aspects must wait for a more detailed experimental and theoretical study.

Evaluation of semi-empirical AM1 and density functional calculations: A closer inspection of the data in Table 1 demonstrates that all three methods applied, including the semi-empirical AM1 method, give very similar geometries. In general, the distances calculated by the AM1 method are a little shorter (ca. 0.05 Å for the cavity dimensions). The optimized geometries of the complexes of axle **10** and macrocycle **9** obtained by DFT and AM1 calculations are also similar with the same hydrogen-bonding patterns. This trend is less evident if their energies are compared (Table 1). Structure **9.1** clearly has the most favored arrangement of nuclei and structure **9.5** the least favored in both treatments. The absolute energy differences are somewhat smaller in the AM1 approach. The energy order of structures **9.2**, **9.3**, and **9.4** is somewhat different for the DFT and semi-empirical approaches. On the other hand, the energy differences between all the structures are quite small so that one should not place too much emphasis on such discrepancies.

Furthermore, earlier examinations of smaller model systems[14] have already shown that the AM1 method is suitable for a qualitative description of two-fold hydrogen bridges. It was also found to be superior to other semi-empirical methods such as the PM3 method, which was developed originally as an improvement on AM1 with regard to hydrogen bonding. At the PM3 level, inaccurate descriptions of the hydrogen bonding were found with O–N distances deviating by up to 0.5 Å. Consequently, for a theoretical approach to larger species, the AM1 method should provide reliable geometries and at least qualitatively correct energies.

Templated synthesis of catenanes and rotaxanes: On the basis of our experience with DFT (some MP2) and AM1 calculations for the macrocycle and rotaxane treated so far, we are confident that larger structures can be reliably described by the AM1 approach and do not require the elaborate DFT treatments. Before studying complete rotaxanes, catenanes, and the trefoil knot, we should briefly mention that the conformation of macrocycle **4**, which bears the cyclohexyl side chains that were omitted in the calculations discussed so far, differs from that of **9** as its dimethylphenyl rings are slightly tilted out of the perpendicular position (Figure 3).[17c,32] However, this difference does not alter any of the conclusions drawn from the calculations performed with **9**.

It comes as no surprise that rotaxane **7** maximizes the number of possible hydrogen-bonding interactions between the axle and the wheel by inverting one of the carbonyl groups of the wheel. This pattern has been described above and one could expect it not to change much just by attaching two stopper groups (Figure 3, top). The same pattern of hydrogen bonds can easily be realized in the templating step of the rotaxane synthesis (Scheme 1). A secondary amide group is capable of forming three hydrogen bonds with a calculated binding energy of 42.8 kJ mol^{-1}, while the only possible competitor, the acid chloride, can only form two hydrogen bonds and thus, in agreement with the experiment,[27] gives a lower binding energy of 15.5 kJ mol^{-1}. The latter complex is thus higher in energy by 27.3 kJ mol^{-1}, as shown in Figure 3. From these considerations, it is clear that semi-axle **11** is threaded into the macrocycle to yield the complex **11·4** by binding of the secondary amide group. Attachment of the second tritylaniline stopper **12** traps the wheel on the axle and leads to the formation of rotaxane **7**.

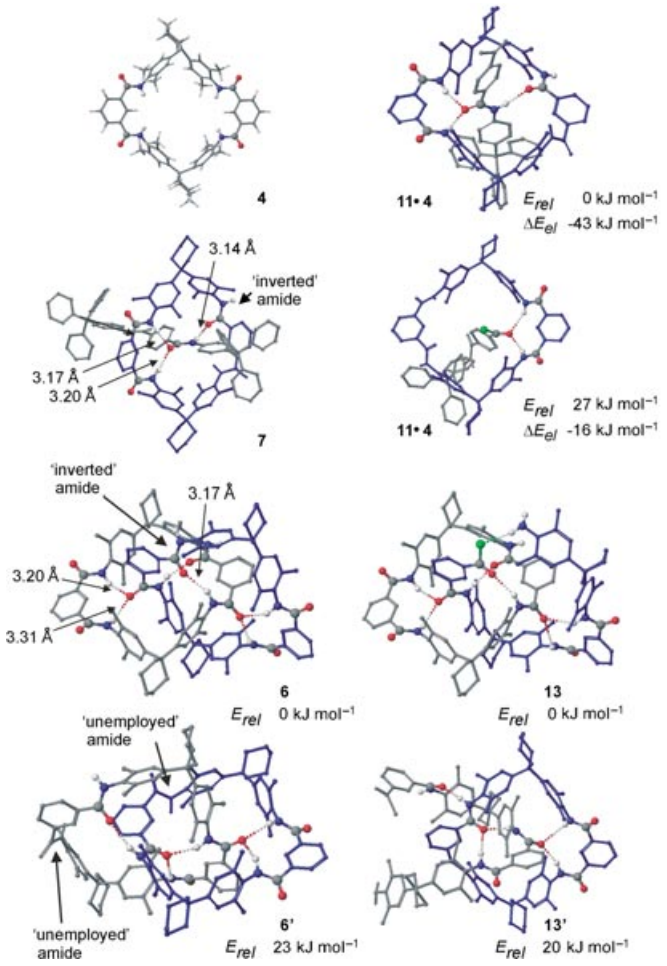

Figure 3. Left (top to bottom): the energetically most favorable structures of macrocycle **4**, rotaxane **7** and catenane **6**. The bottom structure represents conformer **6′** of the catenane, which is higher in energy than **6** by approximately 23 kJ mol^{-1}. Note the common hydrogen-bonding pattern (dotted bonds) of three hydrogen bonds for each pair of macrocyclic host and amide guest. Right: intermediates immediately preceding the products in the templated synthesis of **7** (top) and **6** (bottom). Carbon-centered hydrogen atoms are omitted for clarity. The two components of each structure are shown in different colors (grey and blue). Amide groups involved in hydrogen bonding are shown with CPK colors in ball-and-stick representation. The energies given are relative energies (E_{rel}) calculated at the AM1 level of theory and can be compared only pairwise for structures of the same elemental composition. Electronic energy differences relative to the two components are denoted ΔE_{el}. Some representative lengths of the hydrogen bonds (from donor to acceptor heteroatom) are given for the rotaxane and the catenane.

The situation is somewhat different and more complex for catenane **6**. Here, the two macrocycles bear a total of eight amide groups, which allow for a larger number of hydrogen bonds to be formed simultaneously than in rotaxane **7** or its truncated analogue discussed above. The most stable confor-

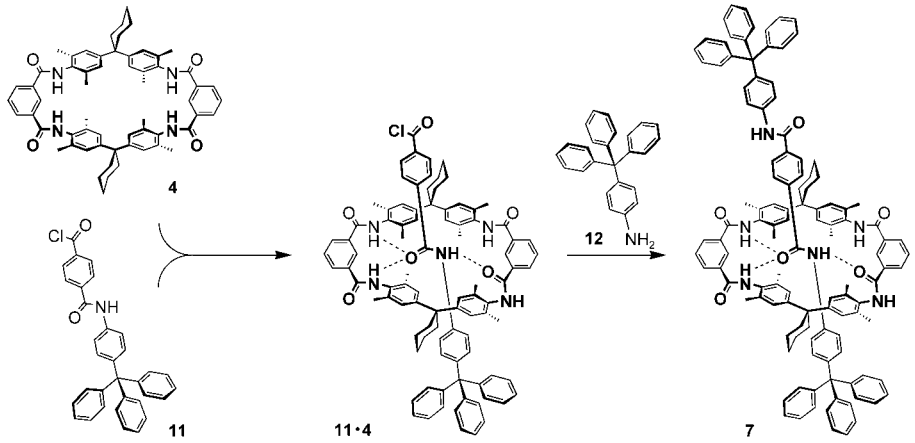

Scheme 1. Template mechanism leading to the formation of rotaxane **7**.

mation found in the calculations is capable of forming a total of six hydrogen bonds, because each wheel serves as the host for one of the amide groups of the other wheel (Figure 3, center). Each of the patterns is analogous to that mediating the binding between the axle and the wheel in rotaxane **7**. A second arrangement is possible that bears a total of five hydrogen bonds (Figure 3, bottom). While the two forked hydrogen bonds in **6** point away from the catenane center in opposite directions, they point in the same direction in the macrocycles of **6′**. This second conformer is less stable than **6** by approximately 23 kJ mol^{-1} in agreement with the crystal structures of analogous catenanes in which the more stable conformer was observed.[9c,33]

However, conformer **6′** is interesting for one reason: while in **6** all amide groups are involved in the hydrogen-bonding pattern, **6′** bears two "unemployed" amide groups. When considering possible intermediates in the synthesis of the catenane, at a late stage, one of the wheels must already be complete, while the second one is still open and needs to be cyclized by the formation of the last amide group while threaded into the first one. In this step, one might expect that the amide opened into an acid chloride and an amine moiety might be unavailable for hydrogen bonding in **6**. Instead, if one of the "unemployed" amide groups in **6′** is opened, the hydrogen-bonding pattern found in this conformer may be retained more or less unchanged. Consequently, it is not clear, a priori, which of these precursors is more stable. We therefore performed calculations on intermediates **13** and **13′**, which are based on ring-opened structures derived from **6** and **6′** by opening one of the amide bonds. Opening other amide bonds would lead to different intermediate conformations, which have been calculated to be less favorable in energy. In agreement with expectation, **13′** bears a hydrogen-bonding pattern similar to that of **6′**. Nevertheless, it is energetically less favorable than **13** by 19.6 kJ mol^{-1} (AM1 calculations), because the hydrogen-bonding pattern in **13** is analogous to that of **6**, so that the number of hydrogen bonds is the same as that in the catenane. The acid chloride moiety in the open wheel is involved in the hydrogen-bonding pattern just like the carbonyl group of the "inverted" amide. An additional, probably weak interaction exists between the terminal NH_2 group of the open wheel and the acid chloride end.

The mechanism of knot formation—a closely analogous hydrogen-bonded template? Owing to its complex structure, a detailed treatment of the trefoil knot **8** is most challenging. Therefore, we start by summarizing some experimental facts.

1) No knot is formed when the extended diamine **1** reacts with isophthaloyl chloride **2**. A knot is found among the products of the reaction only if the pyridine analogue **3** is used. Thus, the pyridine dicarbonyl dichloride is mandatory for successful knot synthesis.
2) Knot formation is not observed when extended diamine **14** bearing a pyridine dicarboxamide reacts with **2**; that is, when the same subunits are used, but their order of use in the synthesis is reversed (Scheme 2). Again, the particular role of the pyridine building block becomes evident.
3) If the flexibility of the extended diamine is increased by introducing additional single bonds into the isophthalic

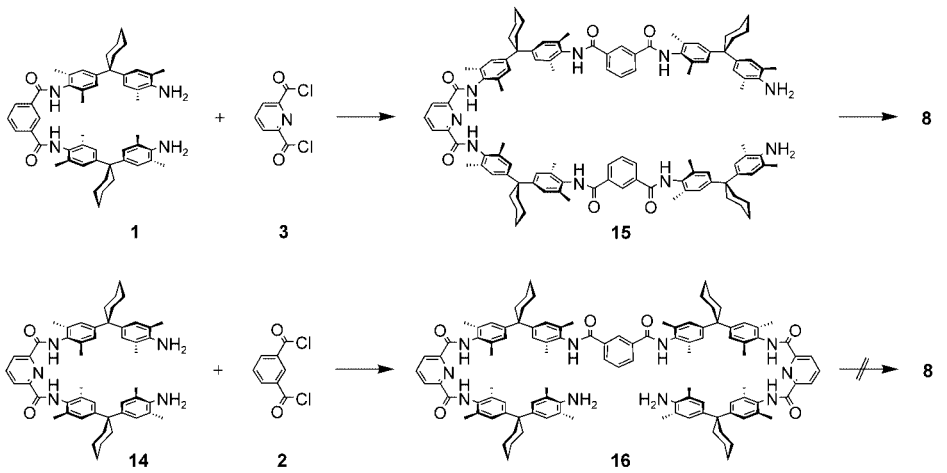

Scheme 2. The pyridine moiety induces curvature through internal hydrogen bonding. Consequently, two different intermediates **15** and **16** are formed depending on which extended diamine is allowed to react with which acid chloride. Only **15** successfully leads to knot formation.

dicarboxamide moiety of **1**, as in **17**–**20** (see below), no knots could be isolated. Seemingly, the additional degrees of freedom prevent a suitable preorganization of the intermediates.

4) Substitution of the pyridine dicarbonyl dichloride **3** at the 5-position is possible, even with larger substituents such as allyloxy, without significant reduction in the yield of the knot, while any substituent in the equivalent position of **1** reduces the yield of the knot or even prevents its formation completely. For example, a methyl group at this position reduces the yield of the knot to less than 5%, while a *tert*-butyl group in the same position results in complete suppression of knot formation.[34]

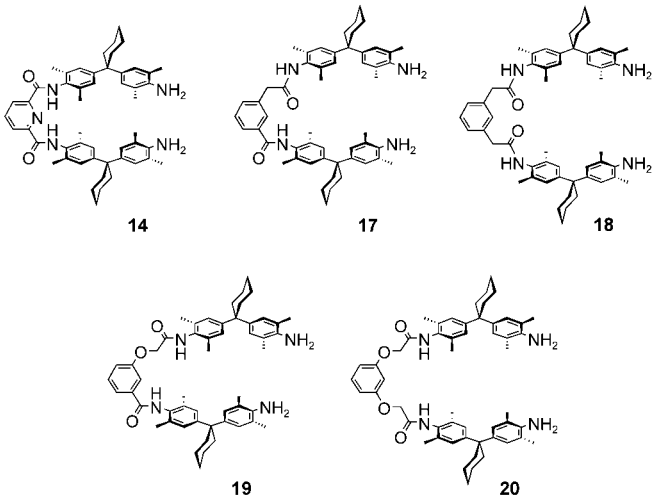

The X-ray crystal structure[12a] of knot **8** provides a rationalization for this finding: while the isophthalic dicarboxamide building blocks are deeply buried inside the knot structure, the pyridine moieties are located at the periphery. During the formation of the knot, substituents in the pyridine rings do not significantly hamper the formation of the intermediates giving rise to the intertwined structure, while substituents in the isophthalic dicarboxamide moieties hinder its formation. These experimental findings underline that not only the presence, but also the exact position of the pyridine subunits is important.

Previous DFT calculations[14] on smaller model systems revealed that the effect of the pyridine moiety is likely to be twofold. On the one hand, the hydrogen bond strength is directly proportional to charge transfer and thus reduced somewhat when isophthalic amides are replaced by the corresponding pyridine derivative. On the other hand, the pyridine's nitrogen atom preorganizes the adjacent amide groups into a geometry that is favorable for the formation of a twofold hydrogen bond to a guest molecule and thus reduces entropic demand when a guest is bound.

With these considerations in mind, one might ask what the particular features of the pyridine–dicarboxamide moiety are. Several earlier publications deal with its ability to form internal hydrogen bonds between the two amide

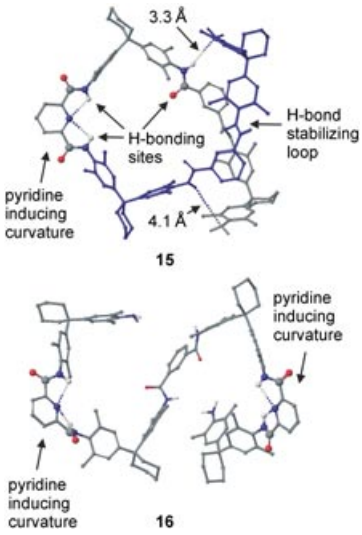

Figure 4. Top: lowest-energy conformation of intermediate **15** which forms a helical loop held together by hydrogen bonds (dotted bonds). Preorganization through the pyridinedicarboxamide group is important. For clarity, the two arms are shown in grey and blue. Three amide groups, which are oriented suitably for binding an extended diamine **1** as the guest, are shown in CPK colors and as a ball-and-stick model. Bottom: lowest energy, S-shaped conformation of intermediate **16**, which bears two pyridine moieties that induce curvature in the wrong parts of the molecules. Carbon-centered hydrogen atoms are omitted for clarity.

protons and the pyridine's nitrogen atom.[35] These hydrogen bonds not only cause the angle between the two arms to contract from the expected 120° to approximately 100°, they also fix the conformation of the amide groups and thus preorganize the arms into a *cisoid* orientation. This is shown in Scheme 2: first, intermediate **15** is formed from **1** and **3** en route to knot **8**. With one pyridine subunit in the center of the molecule, a specific curvature is induced. The intermediate **16**, formed from **2** and **14**, is different. In this case two pyridine moieties are involved and induce curvature where it is not needed, while it is missing in the center of the molecule.

The calculated lowest energy conformations of **15** and **16** (Figure 4) confirm these considerations: while **16** is calculated to have an energetically favorable, but for knot formation, inappropriate S-shaped conformation, the structure of **15** provides an idea as to why just this structure is appropriate as an intermediate in the formation of the knot. A helical loop is formed through internal hydrogen bonding 1) within the pyridinedicarboxamide moiety and 2) between the two arms opposite the pyridine moiety. One real hydrogen bond between two amides of the arms is supported by additional interactions between an amide group of one arm and the NH_2 terminus of the other. However, these interactions are probably rather weak, since distances of 3.3 and 4.1 Å between the functional groups are quite large (Figure 4). Nevertheless, they might help to preorganize the loop. Interestingly, three amide groups within the loop are spatially oriented in a way very similar to the pattern found for rotaxane **7** and catenane **6** so that one might expect that loop-shaped **15** should be able to accommodate an amide guest such as extended diamine **1**. It becomes clear now, why increased flexibility as realized in **17**–**20** prevents knot

formation. A loop-shaped arrangement of more flexible intermediates analogous to **15** will be entropically less favorable, since a larger number of degrees of freedom would have to be constricted. According to a study by Whitesides and co-workers,[36] locking the rotation about one single bond increases the entropic costs by approximately 6.3 kJ mol^{-1}, so that the additional degrees of freedom might well outweigh the stabilization arising from the hydrogen-bonding interactions that preorganize the two arms.

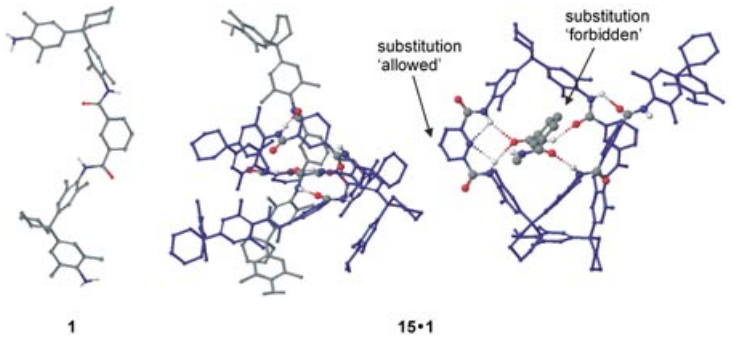

Figure 5. Left: lowest energy conformation of extended diamine **1**. Center: side view of the complex of loop **15** and diamine **1**. Note that the helical loop is conserved in this intermediate with two of the amino termini coming close enough together to react in the required way with pyridine dicarbonyl dichloride. Right: top view of the **15•1** complex. For an unobstructed view of the hydrogen-bonding pattern (dotted bonds), parts of the extended diamine guest have been omitted. Amide groups involved in hydrogen bonding are shown with CPK colors in a ball-and-stick representation. Carbon-centered hydrogen atom are omitted for clarity.

Another feature of the knot is its inherent topological chirality.[37] Since the knot is the only chiral—although racemic—product formed in the reaction of achiral precursors **1** and **3**, the separation of the enantiomers may well serve as evidence[38] for the formation of knots rather than large non-intertwined macrocycles of the same elemental composition. This feature is already reflected in loop-shaped **15**. Since a helix is formed, chirality is already realized in its topology even before the knot is finally formed.

In order to understand the effects of substitution, we need to look at the host–guest complex of loop **15** and extended diamine **1** (Figure 5). In the lowest energy conformer of **15•1**, the helical loop is somewhat contracted in order to accommodate extended diamine **1** as its guest. It is nevertheless still a helical structure, which is likely to be further stabilized by binding the guest, because both molecules are held together by four hydrogen bonds in addition to those found in loop-shaped **15** alone. Again, the hydrogen-bonding pattern found in the structures of catenane **6** and rotaxane **7** is operative and, in addition, a fourth hydrogen bond between the guest and the second arm of the loop is formed. Interestingly, three amide groups within the loop so that substitution at its 5-position would severely distort and likely destroy the loop. Consequently, the interactions between the host and guest would be strongly diminished and knot formation would be expected to be more difficult, if not impossible. Instead, substitution of the pyridine in **15** occurs at the periphery and does not interfere much with the formation of the loop. Note that two amino termini of **1** and **15** are positioned very close to each other in this structure so that they can easily be connected through a second pyridine dicarbonyl dichloride **3**. For the formation of the knot rather than a non-intertwined macrocycle, it is important to connect the correct ends, which is indeed the case if these two ends react with the acid chloride. This mechanistic scenario is depicted in Scheme 3.

However, the arguments presented so far are not conclusive unless they apply analogously to the intermediate directly preceding the final amide bond formation that closes the knot structure. We chose to introduce the arguments

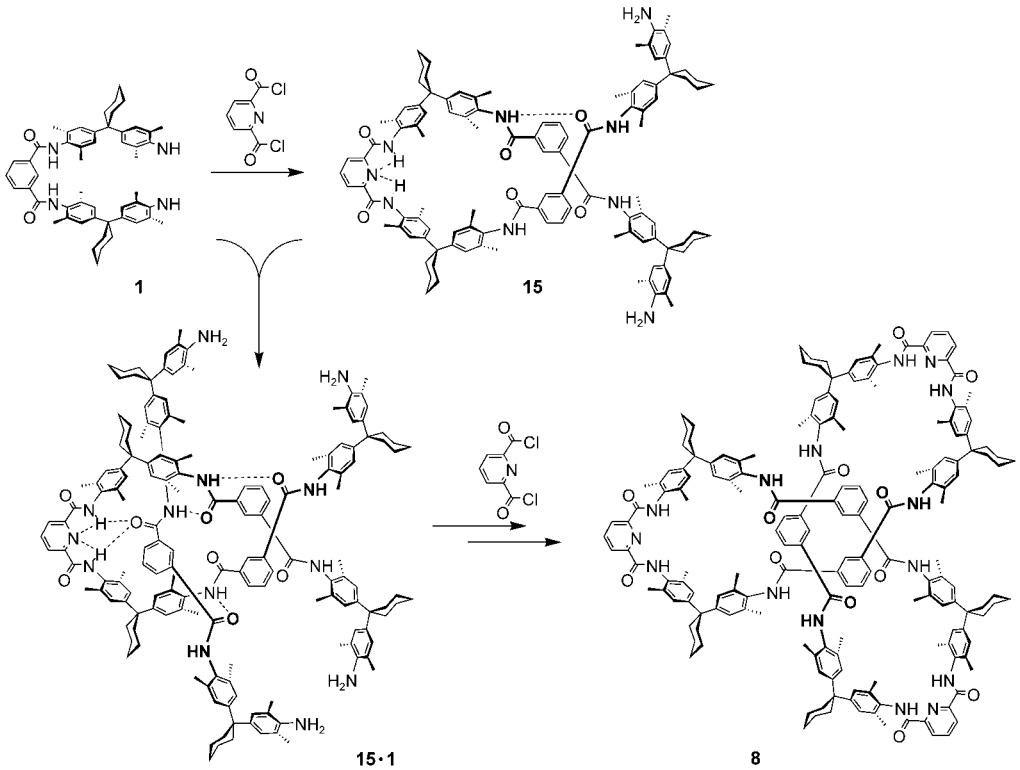

Scheme 3. Template mechanism leading to the formation of knot **8**.

step by step because they are probably easier to follow when the discussion involves less complex structures. However, we finally must put our hypotheses to the test and therefore we performed calculations on the last intermediate and the complete knot (Figure 7). This intermediate, **19**, can be converted into the knot by forming the last of the 12 amide bonds from the acid chloride and amino termini of the molecule. Its lowest energy conformer again supports two typical hydrogen-bonding patterns in which an amide guest is bound by three hydrogen bonds (lower circle in Figure 6). The two reactive ends of the molecule are thus directed towards each other. The amino group can interact with one of the carbonyl groups of the terminal pyridine di-

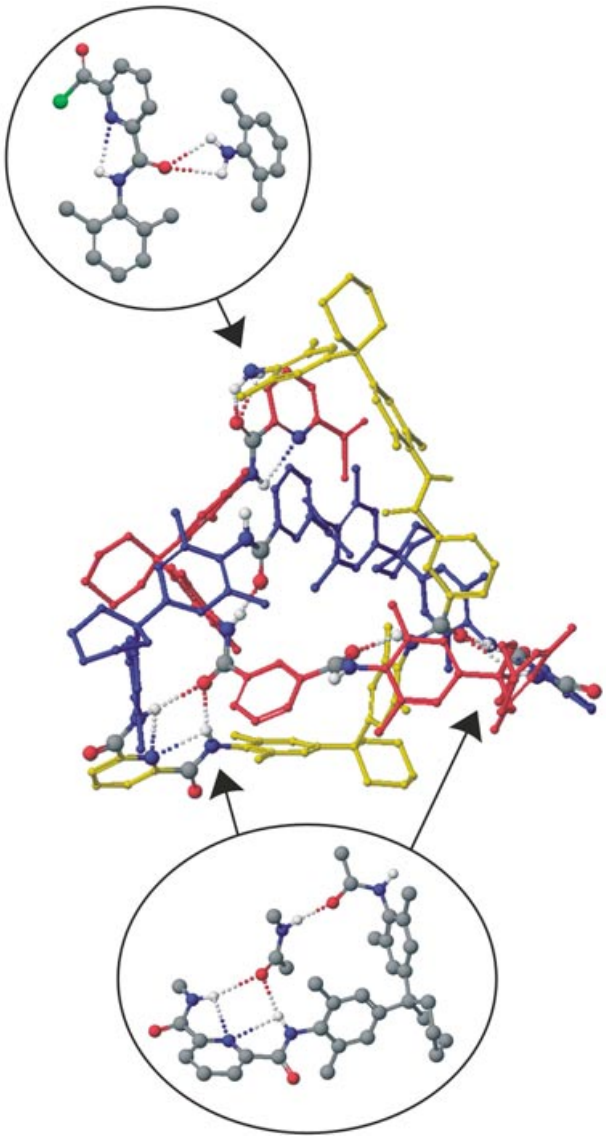

Figure 6. Lowest energy conformation of the immediate precursor **19** for knot formation. The intertwined structure is stabilized by hydrogen-bonding patterns as shown in the two circles. Note that hydrogen bonding also brings the amino and acid chloride termini close together which would be expected to react to form the last amide bond to complete the knot. The three intertwined loops are shown in yellow, blue and red. Amide groups involved in hydrogen bonding are shown in CPK colors and as a ball-and-stick model. Carbon-centered hydrogen atom are omitted for clarity.

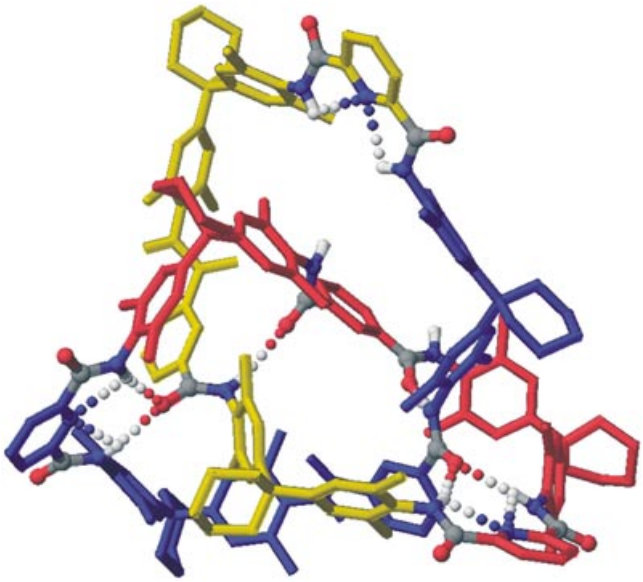

Figure 7. Lowest energy conformer of knot **8**. For clarity, the three intertwined loops are shown in yellow, blue, and red. Amide groups involved in hydrogen bonding are shown in CPK colors and as a ball-and-stick model. Carbon-centered hydrogen atoms are omitted for clarity. Note that the three loops are different with respect to the hydrogen-bonding patterns and their sizes.

carbonyl moiety, as shown in the upper circle in Figure 6. This brings the reactive groups into close proximity so that one can expect them to react efficiently with each other to form the last amide bond and yield knot **8** as the product.

The structure of the knot is depicted in Figure 7. Although the knot has a threefold symmetrical sequence of building blocks, the lowest energy conformer found in the calculations has a lower symmetry. The typical hydrogen-bonding pattern discussed above is found only twice in the knot. The third loop does not form hydrogen bonds with the amide of the adjacent loop. This is quite a remarkable result, which is at least qualitatively in line with the X-ray single-crystal structure, in which only one such pattern was found, while the other two pyridinedicarboxamide groups hydrogen bond to solvent molecules.[12a] It is also in agreement with the finding of different loops in solution which interconvert slowly on the NMR timescale.[38a] The fact that the calculation predicts the hydrogen-bonding pattern to exist in two of the loops, while the crystal structure shows only one such pattern is likely to be due to the presence of competing solvent molecules in the crystal.

Conclusion

In this contribution, we have employed a stepwise approach to more and more complex template effects. Starting with a study of the conformational flexibility of tetralactam macrocycles, rotaxane precursors were investigated by focusing on the hydrogen-bonding pattern that mediates the threading of the axle in the cavity of the wheel. The next level of complexity is a catenane, which is capable of forming a larger number of hydrogen bonds to connect the two wheels. Final-

ly, the most complex structure studied here is the trefoil amide knot and its templated synthesis. From the calculations, a quite general hydrogen-bonding pattern emerges as the basis of all these templated syntheses; it consists of a forked hydrogen bond (referred to as a "twofold hydrogen bond" in reference [14]) between two amide groups of the host and the carbonyl oxygen atom of an amide guest. "Back-bonding" between the amide NH of the guest and one of the carbonyl groups of the host adds a third hydrogen bond, which increases the binding energy and makes secondary amides the preferred guests. In the synthesis of knot **8**, the tetralactam macrocycle is replaced by a helical loop which is "cyclized" by noncovalent interactions rather than by a covalent bond. However, the same functional groups are present in this loop in a favorable orientation to hydrogen bond the appropriate guest needed for knot formation.

Besides revealing this general hydrogen-bonding motif, this study, in line with experimental data, also provides information about the limitations of the structural variations of the knot. Since it is a quite compact architecture, no substitution or functionalization is possible in its interior, while its periphery can be altered in many ways. Also, the degree of flexibility of its components is a major issue as far as the fine and sensitive balance between favorable enthalpic binding interactions and unfavorable entropic effects due to restriction of the degrees of freedom is concerned. Finally, the pyridinedicarboxamide moieties play a pivotal role in the preorganization of the knot precursors and can thus not easily be replaced. These are severe limitations that make the knot a unique species, which is difficult to modify except at the pyridine periphery.

Experiment and theory have been demonstrated to synergistically work together in the analysis of template effects. Even for such complex structures as rotaxanes, catenanes, and trefoil knots, a theoretical approach can help to increase the understanding of the bonding that is important in the template effect. This is important for the design of templates which is still a great challenge for the supramolecular chemist.

Acknowledgements

We thank Dr. Sven Buschbeck, Dr. Anette Hünten, Dr. Oleg Lukin, Dr. Janosch Recker, and Dr. Erik Vogel for sharing with us their experimental experiences. Funding from the Deutsche Forschungsgemeinschaft (SFB 624) and the Fonds der Chemischen Industrie is gratefully acknowledged. C.A.S. thanks the Deutsche Forschungsgemeinschaft for a Heisenberg fellowship and the Fonds der Chemischen Industrie for a Dozentenstipendium.

[1] a) G. Schill, *Catenanes, Rotaxanes and Knots*, Academic Press, New York, **1971**; b) C. O. Dietrich-Buchecker, J.-P. Sauvage, *Chem. Rev.* **1987**, *87*, 795; c) J.-P. Sauvage, *Acc. Chem. Res.* **1990**, *23*, 319; d) R. Hoss, F. Vögtle, *Angew. Chem.* **1994**, *106*, 389; *Angew. Chem. Int. Ed. Engl.* **1994**, *33*, 375; e) R. Jäger, F. Vögtle, *Angew. Chem.* **1997**, *109*, 966; *Angew. Chem. Int. Ed. Engl.* **1997**, *36*, 930; f) S. A. Nepogodiev, J. F. Stoddart, *Chem. Rev.* **1998**, *98*, 1959; g) F. M. Raymo, J. F. Stoddart, *Chem. Rev.* **1999**, *99*, 1043; h) *Molecular Catenanes, Rotaxanes, and Knots* (Eds.: J. P. Sauvage, C. O. Dietrich-Buchecker), Wiley-VCH, Weinheim, **1999**; i) "Catenanes and Interlinked Molecules": A. Rang, C. A. Schalley, in *Encyclopedia of Supramolecular Chemistry* (Eds.: J. L. Atwood, J. W. Steed), Marcel Dekker, New York, **2004**, p. 206; j) "Rotaxanes and Pseudorotaxanes": P. Linnartz, C. A. Schalley, in *Encyclopedia of Supramolecular Chemistry* (Eds.: J. L. Atwood, J. W. Steed), Marcel Dekker, New York, **2004**, p. 1194.

[2] For some reviews on molecular machines, see: a) K. E. Drexler, *Annu. Rev. Biophys. Biomol. Struct.* **1994**, *23*, 377; b) V. Balzani, M. Gómez-López, J. F. Stoddart, *Acc. Chem. Res.* **1998**, *31*, 405; c) J.-P. Sauvage, *Acc. Chem. Res.* **1998**, *31*, 611; d) J.-P. Collin, P. Gaviña, V. Heitz, J.-P. Sauvage, *Eur. J. Inorg. Chem.* **1998**, 1; e) Z. Asfari, J. Vicens, *Macrocyclic Chem.* **2000**, *36*, 103; f) V. Balzani, A. Credi, F. M. Raymo, J. F. Stoddart, *Angew. Chem.* **2000**, *112*, 3484; *Angew. Chem. Int. Ed.* **2000**, *39*, 3348; g) C. A. Schalley, K. Beizai, F. Vögtle, *Acc. Chem. Res.* **2001**, *34*, 465; h) J.-P. Collin, C. O. Dietrich-Buchecker, P. Gaviña, M. C. Jimenez-Molero, J.-P. Sauvage, *Acc. Chem. Res.* **2001**, *34*, 477; i) A. W. Shipway, I. Willner, *Acc. Chem. Res.* **2001**, *34*, 421; j) A. R. Pease, J. O. Jeppesen, J. F. Stoddart, Y. Luo, C. P. Collier, J. R. Heath, *Acc. Chem. Res.* **2001**, *34*, 433; k) R. Ballardini, V. Balzani, A. Credi, M. T. Gandolfi, M. Venturi, *Acc. Chem. Res.* **2001**, *34*, 445; l) C. A. Schalley, *Angew. Chem.* **2002**, *114*, 1583; *Angew. Chem. Int. Ed.* **2002**, *41*, 1513; m) V. Balzani, M. Venturi, A. Credi, *Molecular Devices and Machines: A Journey into the Nanoworld*, Wiley-VCH, Weinheim, **2003**; n) "Artificial Rotary Motors Based on Rotaxanes": T. Felder, C. A. Schalley, in *Highlights in Bioorganic Chemistry* (Eds.: H. Wennemers, C. Schmuck), Wiley-VCH, Weinheim, **2004**, p. 526; m) C. A. Schalley, A. Lützen, M. Albrecht, *Chem. Eur. J.* **2004**, *10*, 1072.

[3] a) A. Credi, V. Balzani, S. J. Langford, J. F. Stoddart, *J. Am. Chem. Soc.* **1997**, *119*, 2679; b) M. Asakawa, P. R. Ashton, V. Balzani, A. Credi, G. Mattersteig, O. A. Matthews, M. Montalti, N. Spencer, J. F. Stoddart, M. Venturi, *Chem. Eur. J.* **1997**, *3*, 1992; c) H. Yu, Y. Luo, K. Beverly, J. F. Stoddart, H.-R. Tseng, J. R. Heath, *Angew. Chem.* **2003**, *115*, 5884; *Angew. Chem. Int. Ed.* **2003**, *42*, 5706.

[4] For general reviews on template effects, see: a) D. H. Busch, N. A. Stephensen, *Coord. Chem. Rev.* **1990**, *100*, 119; b) R. Cacciapaglia, L. Mandolini, *Chem. Soc. Rev.* **1993**, *22*, 221; c) N. V. Gerbeleu, V. B. Arion, J. Burgess, *Template Synthesis of Macrocyclic Compounds*, Wiley-VCH, Weinheim, **1999**; d) *Templated Organic Synthesis* (Eds.: F. Diederich, P. J. Stang), Wiley-VCH, Weinheim, **2000**; e) T. J. Hubin, D. H. Busch, *Coord. Chem. Rev.*, **2000**, *200*, 5; f) B. C. Gibb, *Chem. Eur. J.* **2003**, *9*, 5180.

[5] For reviews on template effects for rotaxane and catenane synthesis, see: a) S. Anderson, H. L. Anderson, J. K. M. Sanders, *Acc. Chem. Res.* **1993**, *26*, 469; b) J.-C. Chambron, C. O. Dietrich-Buchecker, V. Heitz, J.-F. Nierengarten, J.-P. Sauvage, C. Pascard, J. Guilhem, *Pure Appl. Chem.* **1995**, *67*, 233; c) C. Seel, F. Vögtle, *Chem. Eur. J.* **2000**, *6*, 21; d) "How to Thread a String into the Eye of a Molecular Needle: Template-Directed Synthesis of Mechanically Interlocked Molecules": M. Kogej, P. Ghosh, C. A. Schalley, in *Strategies and Tactics in Organic Synthesis* (Ed.: M. Harmata), Academic Press, Oxford, **2004**, p. 171; e) C. A. Schalley, T. Weilandt, J. Brüggemann, F. Vögtle, *Top. Curr. Chem.*, in press.

[6] a) C. O. Dietrich-Buchecker, J.-P. Sauvage, J.-M. Kern, *J. Am. Chem. Soc.* **1984**, *106*, 3043; b) M. Cesario, C. O. Dietrich-Buchecker, A. Edel, J. Guilhem, J.-P. Kintzinger, C. Pascard, J.-P. Sauvage, *J. Am. Chem. Soc.* **1986**, *108*, 6250; c) D. J. Cárdenas, A. Livoreil, J.-P. Sauvage, *J. Am. Chem. Soc.* **1996**, *118*, 11980; d) F. Baumann, A. Livoreil, W. Kaim, J.-P. Sauvage, *Chem. Commun.* **1997**, 35; e) A. Livoreil, J.-P. Sauvage, N. Amaroli, V. Balzani, L. Flamigni, B. Ventura, *J. Am. Chem. Soc.* **1997**, *119*, 12114; f) J.-C. Chambron, J.-P. Sauvage, K. Mislow, A. De Cian, J. Fischer, *Chem. Eur. J.* **2001**, *7*, 4085; g) D. A. Leigh, P. J. Lusby, S. J. Teat, A. J. Wilson, J. K. Y. Wong, *Angew. Chem.* **2001**, *113*, 1586; *Angew. Chem. Int. Ed.* **2001**, *40*, 1538; h) P. Mobian, J.-M. Kern, J.-P. Sauvage, *J. Am. Chem. Soc.* **2003**, *125*, 2016.

[7] a) B. L. Allwood, N. Spencer, H. Shahriari-Zavareh, J. F. Stoddart, D. J. Williams, *J. Chem. Soc. Chem. Commun.* **1987**, 1064; b) P. R. Ashton, I. Iriepa, M. V. Reddington, N. Spencer, A. M. Z. Slawin, J. F. Stoddart, D. J. Williams, *Tetrahedron Lett.* **1994**, *35*, 4835; c) M. Asakawa, P. R. Ashton, S. E. Boyd, C. L. Brown, S. Menzer, D.

Pasini, J. F. Stoddart, M. S. Tolley, A. J. P. White, D. J. Williams, P. G. Wyatt, *Chem. Eur. J.* **1997**, *3*, 463.

[8] a) A. G. Kolchinski, D. H. Busch, N. W. Alcock, *J. Chem. Soc. Chem. Commun.* **1995**, 1289; b) P. R. Ashton, P. J. Campbell, E. J. T. Chrystal, P. T. Glink, S. Menzer, D. Philp, N. Spencer, J. F. Stoddart, P. A. Tasker, D. J. Williams, *Angew. Chem.* **1995**, *107*, 1997; *Angew. Chem. Int. Ed. Engl.* **1995**, *34*, 1865; c) P. R. Ashton, E. J. T. Chrystal, P. T. Glink, S. Menzer, C. Schiavo, J. F. Stoddart, P. A. Tasker, D. J. Williams, *Angew. Chem.* **1995**, *107*, 2001; *Angew. Chem. Int. Ed. Engl.* **1995**, *34*, 1869; d) P. T. Glink, C. Schiavo, J. F. Stoddart, D. J. Williams, *Chem. Commun.* **1996**, 1483; e) P. R. Ashton, A. N. Collins, M. C. T. Fyfe, S. Menzer, J. F. Stoddart, D. J. Williams, *Angew. Chem.* **1997**, *109*, 760; *Angew. Chem. Int. Ed. Engl.* **1997**, *36*, 735; f) F. G. Gatti, D. A. Leigh, S. A. Nepogodiev, A. M. Z. Slawin, S. J. Teat, J. K. Y. Wong, *J. Am. Chem. Soc.* **2001**, *123*, 5983.

[9] a) F. Vögtle, S. Meier, R. Hoss, *Angew. Chem.* **1992**, *104*, 1628; *Angew. Chem. Int. Ed. Engl.* **1992**, *31*, 1619; b) S. Ottens-Hildebrandt, S. Meier, W. Schmidt, F. Vögtle, *Angew. Chem.* **1994**, *106*, 1818; *Angew. Chem. Int. Ed. Engl.* **1994**, *33*, 1767; c) S. Ottens-Hildebrandt, M. Nieger, K. Rissanen, J. Rouvinen, S. Meier, G. Harder, F. Vögtle, *J. Chem. Soc. Chem. Commun.* **1995**, 777; d) H. Adams, F. J. Carver, C. A. Hunter, *J. Chem. Soc. Chem. Commun.* **1995**, 809; e) A. G. Johnston, D. A. Leigh, R. J. Pritchard, M. D. Deegan, *Angew. Chem.* **1995**, *107*, 1324; *Angew. Chem. Int. Ed. Engl.* **1995**, *34*, 1209; f) Y. Geerts, D. Muscat, K. Müllen, *Macrmol. Chem. Phys.* **1995**, *196*, 3425; g) D. A. Leigh, K. Moody, J. P. Smart, K. J. Watson, A. M. Z. Slawin, *Angew. Chem.* **1996**, *108*, 326; *Angew. Chem. Int. Ed. Engl.* **1996**, *35*, 306; h) D. Muscat, A. Witte, W. Köhler, K. Müllen, Y. Geerts, *Macromol. Rapid Commun.* **1997**, *18*, 233; i) T. Dünnwald, A. H. Parham, F. Vögtle, *Synthesis* **1998**, *3*, 339; j) T. Schmidt, R. Schmieder, W. M. Müller, B. Kiupel, F. Vögtle, *Eur. J. Org. Chem.* **1998**, 2003; k) A. H. Parham, R. Schmieder, F. Vögtle, *Synlett* **1999**, 1887.

[10] a) G. M. Hübner, J. Gläser, C. Seel, F. Vögtle, *Angew. Chem.* **1999**, *111*, 395; *Angew. Chem. Int. Ed.* **1999**, *38*, 383; b) C. Reuter, W. Wienand, G. M. Hübner, C. Seel, F. Vögtle, *Chem. Eur. J.* **1999**, *5*, 2692; c) C. Reuter, F. Vögtle, *Org. Lett.* **2000**, *2*, 593; d) G. M. Hübner, C. Reuter, C. Seel, F. Vögtle, *Synthesis* **2000**, 103; e) P. Ghosh, O. Mermagen, C. A. Schalley, *Chem. Commun*, **2002**, 2628; f) J. A. Wisner, P. D. Beer, N. G. Berry, B. Tomapatanaget, *Proc. Natl. Acad. Sci. USA* **2002**, *99*, 4983; g) J. A. Wisner, P. D. Beer, M. G. B. Drew, M. R. Sambrook *J. Am. Chem. Soc.* **2002**, *124*, 12469.

[11] a) C. A. Hunter, *J. Chem. Soc. Chem. Commun.* **1991**, 749; b) C. A. Hunter, *J. Am. Chem. Soc.* **1992**, *114*, 5303.

[12] a) O. Safarowsky, M. Nieger, R. Fröhlich, F. Vögtle, *Angew. Chem.* **2000**, *112*, 1699; *Angew. Chem. Int. Ed.* **2000**, *39*, 1616; b) F. Vögtle, A. Hünten, E. Vogel, S. Buschbeck, O. Safarowsky, J. Recker, A. Parham, M. Knott, W. M. Müller, U. Müller, Y. Okamoto, T. Kubota, W. Lindner, E. Francotte, S. Grimme, *Angew. Chem.* **2001**, *113*, 2534; *Angew. Chem. Int. Ed.* **2001**, *40*, 2468; c) J. Recker, W. M. Müller, U. Müller, T. Kubota, Y. Okamoto, M. Nieger, F. Vögtle, *Chem. Eur. J.* **2002**, *8*, 4434.

[13] Several theoretical studies of related amide-based rotaxanes and catenanes are available that focus on the motions in such species: a) M. S. Deleuze, D. A. Leigh, F. Zerbetto, *J. Am. Chem. Soc.* **1999**, *121*, 2364; b) D. A. Leigh, A. Troisi, F. Zerbetto, *Angew. Chem.* **2000**, *112*, 358; *Angew. Chem. Int. Ed.* **2000**, *39*, 350; c) C.-A. Fustin, D. A. Leigh, P. Rudolf, D. Timpel, F. Zerbetto, *ChemPhysChem* **2000**, *1*, 97; d) G. Brancato, F. Coutrot, D. A. Leigh, A. Murphy, J. K. Y. Wong, F. Zerbetto, *Proc. Natl. Acad. Sci. USA* **2002**, *99*, 4967.

[14] W. Reckien, S. Peyerimhoff, *J. Phys. Chem. A* **2003**, *107*, 9634.

[15] a) S. J. Weiner, P. A. Kollman, D. A. Case, U. C. Singh, G. Alagona, S. Profeta, P. Weiner, *J. Am. Chem. Soc.* **1984**, *106*, 765; b) S. J. Weiner, P. A. Kollman, N. T. Nguyen, D. A. Case, *J. Comput. Chem.* **1986**, *7*, 230; c) D. M. Ferguson, P. A. Kollman, *J. Comput. Chem.* **1991**, *12*, 620.

[16] Schrödinger, Inc., 1500 SW First Avenue, Suite 1180, Portland, OR 97201 (USA). Also, see: a) F. Mohamadi, N. G. Richards, W. C. Guida, R. Liskamp, C. Caulfield, G. Chang, T. Hendrickson, W. C. Still, *J. Comput. Chem.* **1990**, *11*, 440; b) D. Q. McDonald, W. C. Still, *Tetrahedron Lett.* **1992**, *33*, 7743.

[17] a) C. A. Schalley, G. Silva, C. F. Nising, P. Linnartz, *Helv. Chim. Acta* **2002**, *85*, 1578; b) X.-y. Li, J. Illigen, M. Nieger, S. Michel, C. A. Schalley, *Chem. Eur. J.* **2003**, *9*, 1332; c) P. Linnartz, S. Bitter, C. A. Schalley, *Eur. J. Org. Chem.* **2003**, 4819; d) P. Linnartz, C. A. Schalley, *Supramol. Chem.* **2004**, *16*, 263.

[18] CaChe 5.0 for Windows, Fujitsu Ltd., Krakow, Poland, **2001**.

[19] Gaussian 98 (Revision A.7), M. J. Frisch, G. W. Trucks, H. B. Schlegel, G. E. Scuseria, M. A. Robb, J. R. Cheeseman, V. G. Zakrzewski, J. A. Montgomery, Jr., R. E. Stratmann, J. C. Burant, S. Dapprich, J. M. Millam, A. D. Daniels, K. N. Kudin, M. C. Strain, O. Farkas, J. Tomasi, V. Barone, M. Cossi, R. Cammi, B. Mennucci, C. Pomelli, C. Adamo, S. Clifford, J. Ochterski, G. A. Petersson, P. Y. Ayala, Q. Cui, K. Morokuma, D. K. Malick, A. D. Rabuck, K. Raghavachari, J. B. Foresman, J. Cioslowski, J. V. Ortiz, B. B. Stefanov, G. Liu, A. Liashenko, P. Piskorz, I. Komaromi, R. Gomperts, R. L. Martin, D. J. Fox, T. Keith, M. A. Al-Laham, C. Y. Peng, A. Nanayakkara, C. Gonzalez, M. Challacombe, P. M. W. Gill, B. G. Johnson, W. Chen, M. W. Wong, J. L. Andres, M. Head-Gordon, E. S. Replogle, J. A. Pople, Gaussian, Inc., Pittsburgh, PA, **1998**.

[20] R. Ahlrichs, M. Bär, M. Häser, H. Horn, C. Kömel, *Chem. Phys. Lett.* **1989**, *162*, 165

[21] A. D. Becke, *J. Chem. Phys.* **1993**, *98*, 5648; b) P. J Stephens, F. J. Devlin, C. F. Chabalowski, J. M. Frisch, *J. Chem. Phys.* **1993**, *98*, 11623.

[22] a) A. D. Becke, *Phys. Rev. A* **1988**, *38*, 3098; b) J. P. Perdew, Y. Wang, *Phys. Rev. B* **1986**, *33*, 8822.

[23] a) O. Treutler, R. Ahlrichs, *J. Chem. Phys.* **1995**, *102*, 346; b) K. Eichkorn, O. Treutler, H. Oehm, M. Häser, R. Ahlrichs, *Chem. Phys. Lett.* **1995**, *240*, 283; c) K. Eichkorn, F. Weigend, O. Treutler, R. Ahlrichs, *Theor. Chem. Acc.* **1997**, *97*, 119.

[24] A. D. Becke, *J. Chem. Phys.* **1993**, *98*, 1372.

[25] S. F. Boys, F. Bernardi, *Mol. Phys.* **1970**, *19*, 553.

[26] A. Klamt, G. Schüürmann, *J. Chem. Soc. Perkin Trans. 2* **1993**, 799.

[27] Rotaxanes with such axle center pieces have previously been prepared and studied experimentally: C. Seel, A. H. Parham, O. Safarowsky, G. M. Hübner, F. Vögtle, *J. Org. Chem.* **1999**, *64*, 7236.

[28] a) F. Weigend, M. Häser, *Theor. Chem. Acc.* **1997**, *97*, 331; b) F. Weigend, M. Häser, H. Patzelt, R. Ahlrichs, *Chem. Phys. Lett.* **1998**, *294*, 143.

[29] C. Reuter, C. Seel, M. Nieger, F. Vögtle, *Helv. Chim. Acta* **2000**, *83*, 630.

[30] J. Kang, J. Rebek, Jr., *Nature* **1996**, *382*, 239.

[31] Note that the BSSE can only be calculated for complexes in the gas phase (i.e. with $\varepsilon = 1.0$) and amounts to 25.5 kJ mol^{-1} for **10·9.2** and 31.4 kJ mol^{-1} for **10·9.5**. For the calculations of the binding energies, we assume that it does not change much with the dielectric constant.

[32] P. Ghosh, D. Haase, W. Saak, A. Lützen, C. A. Schalley, unpublished results.

[33] A. Mohry, F. Vögtle, M. Nieger, H. Hupfer, *Chirality* **2000**, *12*, 76. For the results of theoretical studies on different amide-type catenanes with a similar hydrogen bonding pattern, see reference [13a].

[34] a) A. Hünten, Ph.D. Thesis, University of Bonn, **2000**; b) S. Buschbeck, Ph.D. Thesis, University of Bonn, **2002**; c) J. Recker, Ph.D. Thesis, University of Bonn, **2002**.

[35] a) C. A. Hunter, D. H. Purvis, *Angew. Chem.* **1992**, *104*, 779; *Angew. Chem. Int. Ed. Engl.* **1992**, *31*, 792; b) Y. Hamuro, S. J. Geib, A. D. Hamilton, *Angew. Chem.* **1994**, *106*, 465; *Angew. Chem. Int. Ed. Engl.* **1994**, *33*, 446; c) C. A. Hunter, L. D. Sarson, *Angew. Chem.* **1994**, *106*, 2424; *Angew. Chem. Int. Ed. Engl.* **1994**, *33*, 2313; d) V. Berl, I. Huc, R. G. Khoury, M. J. Krische, J.-M. Lehn, *Nature* **2000**, *407*, 720; e) V. Berl, M. J. Krische, I. Huc, J.-M. Lehn, M. Schmutz, *Chem. Eur. J.* **2000**, *6*, 1938; d) A. Affeld, G. M. Hübner, C. Seel, C. A. Schalley, *Eur. J. Org. Chem.* **2001**, 2877.

[36] a) M. Mammen, E. I. Shakhnovich, J. M. Deutch, G. M. Whitesides, *J. Org. Chem.* **1998**, *63*, 3821. Also, see: b) B. M. O'Leary, T. Szabo, N. Svenstrup, C. A. Schalley, A. Lützen, M. Schäfer, J. Rebek, Jr., *J. Am. Chem. Soc.* **2001**, *123*, 11519.

[37] For reviews on topological chirality, see: a) J.-C. Chambron, C. O. Dietrich-Buchecker, J.-P. Sauvage, *Top. Curr. Chem.* **1993**, *165*, 131; b) K. Mislow, *Top. Stereochem.* **1999**, 1; c) C. Reuter, R. Schmieder, F. Vögtle, *Pure Appl. Chem.* **2000**, *72*, 2233.

[38] Further evidence comes from crystal structure analysis, NMR experiments, and mass spectrometry. See: a) O. Lukin, W. M. Müller, U. Müller, A. Kaufmann, C. Schmidt, J. Leszczynski, F. Vögtle, *Chem. Eur. J.* **2003**, *9*, 3507; b) C. A. Schalley, J. Hoernschemeyer, G. Silva, X.-y. Li, P. Weis, *Int. J. Mass Spectrom.* **2003**, *228*, 373; c) C. A. Schalley, P. Ghosh, M. Engeser, *Int. J. Mass Spectrom.* **2004**, *232–233*, 249.

Received: April 14, 2004
Published online: August 17, 2004

